Device Engineering for Highly Efficient Top-Illuminated Organic Solar Cells with Microcavity Structures

Hao-Wu Lin, Si-Wen Chiu, Li-Yen Lin, Zheng-Yu Hung, Yi-Hong Chen, Francis Lin, and Ken-Tsung Wong**

Organic solar cells (OSCs) as possible next-generation solar energy-harvesting devices have attracted considerable research interest owing to their low-energy consumption in fabrication, potential mechanical flexibility, and low-cost manufacturing.[1–4] Recently, the power-conversion efficiencies (PCEs) of small-molecule organic solar cells (SMOSCs) have been significantly improved, primarily due to the incorporation of new donor materials,[5–9] the sophistication of device structures,[10] and better control of active-layer morphology.[11,12] Very recently, we reported a donor–acceptor–acceptor (D–A–A) molecular configuration to construct donor molecules for SMOSCs, and the planar-mixed heterojunction (PMHJ) devices based on these D–A–A donors have demonstrated PCEs in excess of 6%.[13,14] In these works and also most of the OSCs reported in the literature, indium tin oxide (ITO) was exclusively used as the standard anode due to its excellent transparency and conductivity. However, there also exist several long-standing drawbacks for ITO such as 1) its brittle nature, that is unsuitable for flexible cells;[15] 2) its relatively low conductivity as compared to metal electrodes[16–18] and; 3) the scarcity of indium, which makes the cost of ITO uncompetitive.[19] As such, significant research endeavours have been dedicated to pursuing alternative electrode materials to ITO such as metals,[20,21] carbon nanotubes,[22–24] reduced graphene oxide,[25] and silver nanowires.[17] In particular, ITO-free microcavity devices utilizing optically thick and semitransparent metal layers as both the anode and cathode have demonstrated PCEs of ≈1–3%.[21,26–30] Due to the more complicated optical structures in these microcavity devices compared to conventional ITO cells, a large improvement of short-circuit current densities (J_{sc}) and PCEs can been realized by fine-tuning the thin metal layers[21,27,28] as well as the thicknesses of organic active layers[31] and capping layers.[26,27,29,32,33] Although these results disclosed a promising way to realize ITO-free OSCs with optically thin metal in-coupling electrodes, their efficiencies were still much lower than those of their ITO-based counterparts. In this letter, we model and experimentally demonstrate highly efficient SMOSCs based on microcavity structures with PCEs exceeding 5%. Specifically, the device structure was designed with the following characteristics: i) the thicknesses of the organic active layers were kept the same as their optimized values in ITO-based cells for the best carrier transportation properties;[14] ii) the optical-field distribution was tuned by simultaneous optimization of the in-cell optical spacer layer and out-of-cell capping layer; iii) very thin solar-absorbing active layers (total thickness = 54 nm) were used, to allow a maximum interaction/resonance of in-cell and out-of-cell optical structures; iv) molybdenum trioxide (MoO_3) films were adopted as the in-cell optical spacer due to their excellent hole-transporting properties.[34,35] The PMHJ device structures (**Figure 1**a) were configured as: glass or polyethylene terephthalate (PET)/Ag (150 nm)/MoO_3 (spacer layer)/**DTDCTP** (2-{[2-(5-*N*,*N*-di(*p*-tolyl)aminothiophen-2-yl)-pyrididin-5-yl]methylene}malononitrile, Figure 1b) (7 nm)/**DTDCTP**:C_{70} (1:1, by volume, 40 nm)/C_{70} (Figure 1c) (7 nm)/2,9-dimethyl-4,7-diphenyl-1,10-phenanthroline (BCP) (10 nm)/Ag (12.5 nm)/LiF or MoO_3 (capping layer). A home-built panchromatic optical field simulation program coded in Matlab based on a transfer matrix method was used to model and optimize device performance prior to fabrication.[36]

First, microcavity cells without capping layers were modelled and fabricated. **Figure 2** shows the optical field distributions in

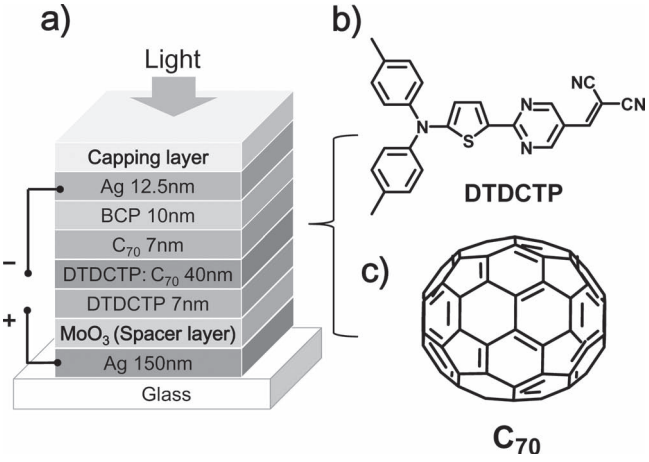

Figure 1. a) Device structure. b) Molecular structure of **DTDCTP**. c) Molecular structure of C_{70}.

Prof. H.-W. Lin, S.-W. Chiu, Z.-Y. Hung, Y.-H. Chen
Department of Materials Science and Engineering
National Tsing Hua University
No. 101, Section 2, Kuang-Fu Road,
Hsinchu 30013, Taiwan
E-mail: hwlin@mx.nthu.edu.tw
L.-Y. Lin, F. Lin, Prof. K.-T. Wong
Department of Chemistry
National Taiwan University
No. 1, Sec. 4, Roosevelt Road, Taipei 10617, Taiwan
E-mail: kenwong@ntu.edu.tw

DOI: 10.1002/adma.201200487

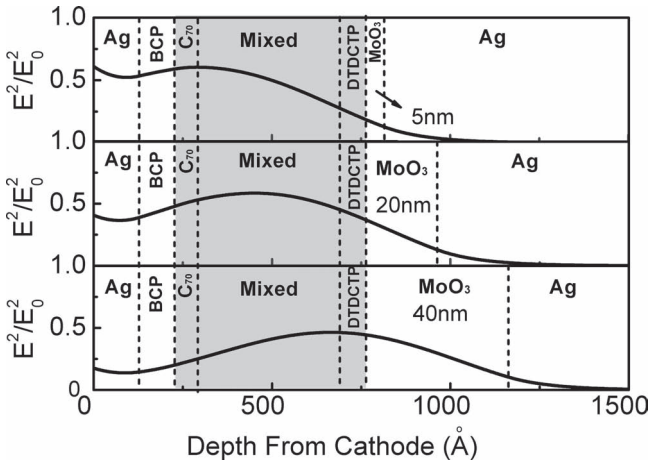

Figure 2. Calculated optical-field distributions at the wavelength of 590 nm. The gray area indicates the solar-absorbing active layers.

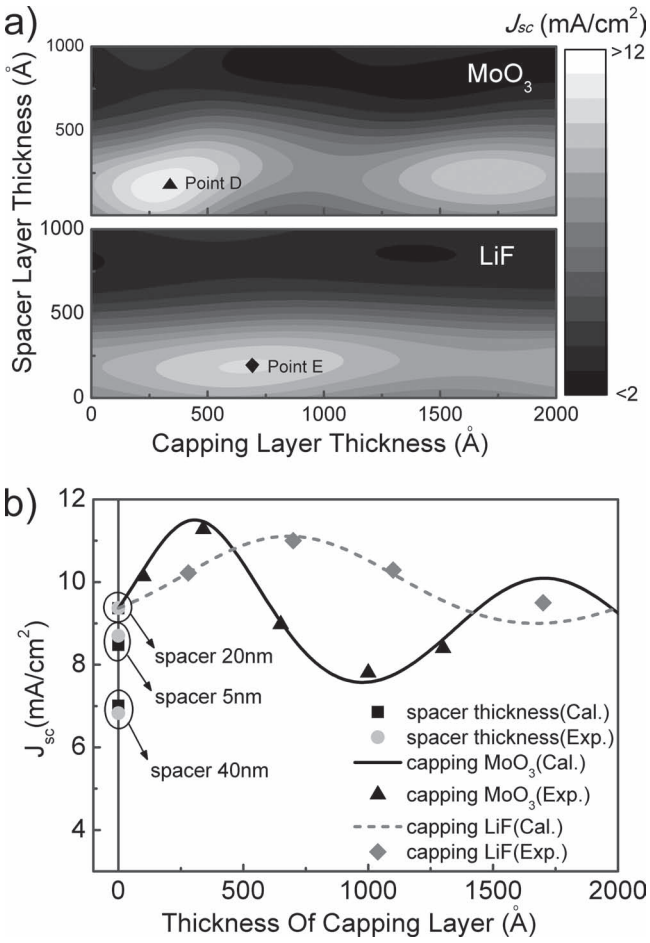

Figure 3. a) Simulated J_{sc} as a function of spacer and capping layer thickness. b) Modelled and experimental J_{sc}. Filled squares (■) and filled circles (●): calculated and experimental J_{sc}, respectively, of devices with different thicknesses of spacer layers. Solid lines and filled triangles (▲): calculated and experimental J_{sc}, respectively, of devices with different thicknesses of MoO_3 capping layer. Dashed line and filled diamond (◆): calculated and experimental J_{sc}, respectively, of devices with different thicknesses of LiF capping layer. Cal.: calculated. Exp.: experimental.

cells with different thicknesses for the spacer layer (Device **A**: 5 nm, Device **B**: 20 nm, Device **C**: 40 nm; for detailed device structures see Supporting Information). Apparently, one can locate the optical field maximum to the bulk heterojunction (BHJ) layer through controlling the thickness of the spacer layer, thus enhancing photon harvesting in the very thin active layers. Device **B**, of which the thickness of the spacer layer was optimized, showed a maximum J_{sc} of 9.4 mA cm^{-2} and thus a maximum PCE of 4.3% under AM 1.5G 1 sun (100 mW cm^{-2}) simulated solar illumination. As shown in **Figure 3**b, the experimental J_{sc} values are in excellent agreement with the simulated results, indicating that our simulation program can mimic the cell performance well. The fill factor (FF) and open-circuit voltage (V_{oc}) were approximately the same in these devices because of the same configuration in the active layers and good transporting properties of MoO_3 which may not significantly alter the electrical properties in this thickness range.

To evaluate the effect of capping layers on the performance of microcavity cells, two model materials with high (n ~ 2.1, MoO_3) and low (n ~ 1.4, LiF) refractive index were then individually incorporated into the devices with an optimized thickness for the MoO_3 spacer layer. MoO_3 and LiF were chosen owing to their good transparency across the whole solar spectrum (spectroscopic ellipsometer measured optical constants of vacuum deposited MoO_3 and LiF and absorption spectrum of MoO_3 thin film were shown in Supporting Information). These two types of devices also enable us to investigate the relationship between the refractive indices of capping layers and the device performance. Figure 3a shows the simulated J_{sc} as a function of the thicknesses of the spacer layer and capping layers. Interestingly, the maximum J_{sc} (Point **D**) attainable in the cell with a MoO_3 capping layer is larger than that (Point **E**) in the LiF-based cell, implying that as long as the capping layer materials are highly transparent in the solar spectrum range, the higher the refractive index, the higher efficiency would be obtained if their thicknesses have been optimized. The simulated results may provide a useful guideline for the selection of capping layer materials in future optical designs of microcavity structures. As shown in Figure 3b, the J_{sc} for the practical cells match the simulated curves exceptionally well. In addition, it is revealed that the J_{sc} values are highly dependent on not only the capping layer materials but also the thicknesses of the capping layers. The optimized thicknesses for the capped MoO_3 layer and LiF layer were 34 nm (Device **D**) and 70 nm (Device **E**), respectively. Under AM 1.5G 1 sun simulated solar irradiation, devices **D** and **E** gave higher J_{sc} of 11.3 and 10.9 mA cm^{-2} than the device **B**, thus yielding impressively high PCE of 5.5% and 5.1%, respectively. **Figure 4** depicts J–V characteristics and external quantum efficiency (EQE) spectra of devices **B**, **C**, and **D**. It is worthy to note that the FF and V_{oc} values are almost as the same as those offered in ITO-based cells, indicating that only the optical fields have been manipulated while the electrical properties are not considerably varied in our optical-engineering approach reported in this letter. As shown in the inset of Figure 4, the EQE spectra change largely with

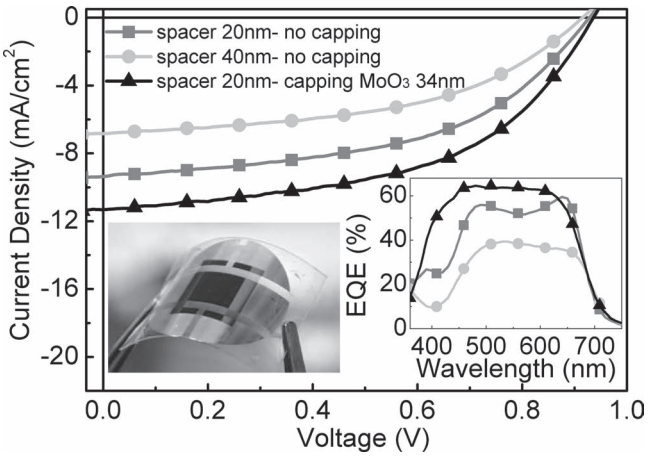

Figure 4. *J–V* characteristics of microcavity devices. Inset left: Photograph of a top-illuminated device on a flexible PET substrate. Inset right: EQE spectra of microcavity devices. Filled squares (■): device with a 20 nm spacer layer and without capping layers. Filled circles (●): device with a 40 nm spacer layer and without capping layers. Filled triangles (▲): device with a 20 nm spacer layer and 34 nm MoO_3 capping layer.

adopting different device structures, which can be attributed to the microcavity effect that influences the wavelength dependent optical field distribution inside the devices.

Since the electrodes used in the top-illuminated microcavity structure are substrate-insensitive, proof-of-concept flexible devices **F** (area ≈ 5 mm^2) and **G** (area ≈ 36 mm^2) with the same device structure as the device **D** were fabricated on PET to demonstrate the benefit of this device configuration. The performance parameters and photograph of the flexible devices are summarized and shown in **Table 1** and inset of Figure 4, respectively. Compared to the devices on the glass substrate, only limited losses in J_{sc} and FF were observed. This may be ascribed to rugged surface morphology of the PET substrate which could cause some additional carrier losses. In principle, we believe that cells on smooth flexible substrates should have similar performance as cells on glass substrates. Further improvement in flexible top-illuminated microcavity devices could be achieved by utilizing smoother plastic substrates or substrates with smoothing barrier layers.

In conclusion, SMOSCs with microcavity structures utilizing very thin solar-absorbing active layers have been simulated and fabricated. By carefully fine-tuning the in-cell spacer layer and out-of-cell capping layer, highly efficient top-illuminated ITO-free solar cells were demonstrated on glass and flexible PET substrates with efficiencies of up to 5.5% and 5%, respectively. The efficiency values are among the highest reported ITO-free organic solar cells on glass and flexible substrates.[37] The high efficiencies are primarily attributed to the electrically optimized thin active layers and panchromatic simulation program designed device structures incorporating favourable materials with good electrical and optical properties. We believe the methodology reported here can also be applied to general top-illuminated OSCs using either polymers or small molecules as solar absorbing materials.

Table 1. Performance parameters of devices.

Device	J_{sc} [mA cm^{-2}]	V_{oc} [V]	FF	PCE [%]
Device A	8.7	0.89	0.48	3.7
Device B	9.4	0.93	0.50	4.3
Device C	6.8	0.92	0.53	3.3
Device D	11.3	0.94	0.52	5.5
Device E	10.9	0.92	0.51	5.1
Device F	10.3	0.94	0.51	5.0
Device G	9.9	0.93	0.52	4.8

Experimental Section

Organic compounds including synthesized **DTDCTP**, purchased fullerene C_{70}, and 2,9-dimethyl-4,7-diphenyl-1,10-phenanthroline (BCP), were subjected to purification at least once by temperature-gradient sublimation before use in this study. The organic, metal oxide thin films, salts, and metal electrodes were deposited on precleaned substrates in a high vacuum chamber with base pressure ≈ 1×10^{-6} Torr. The deposition was performed at rate of 1–2 Å with the substrate held at room temperature. Thicknesses were monitored using a crystal oscillator during deposition and were verified later with spectroscopic ellipsometry. The active area of the cells had an average size of 5 mm^2. Flexible device **G** had an average size of 36 mm^2. Flexible devices were fabricated on PET substrate. Devices were measured in dry nitrogen atmosphere. Current density–voltage characteristics were measured with a SourceMeter Keithley 2636A under illumination of AM 1.5G solar light from a xenon lamp solar simulator (Abet Technologies). The incident light intensity was calibrated as 100 mW cm^{-2} by a monocrystalline silicon reference cell with KG-5 filter. The external quantum efficiency spectra were taken by illuminating chopped monochromatic light with a continuous-wave bias white light (from halogen lamp) on the solar cells. The photocurrent signals were extracted with lock-in technique using a current preamplifier (Stanford Research System) followed by a lock-in amplifier (AMETEK). The external quantum efficiency measurement is fully computer controlled and the intensity of monochromatic light is carefully calibrated with optical power meter (Ophir Optronics). Ellipsometry measurements were carried out with J. A. Woollam Inc. V-VASE variable-angle spectroscopic ellipsometer. Simulation program is coded with Matlab software (The MathWorks, Inc.) and performed with dual-core Intel-CPU personal computer. Absorption spectra were obtained by spectrometer with reflectance accessory (PerkinElmer).

Supporting Information

Supporting Information is available from the Wiley Online Library or from the author.

Acknowledgements

S. W. Chiu and L. Y. Lin contributed equally to this work. The authors would like to acknowledge the financial support from National Science Council of Taiwan (NSC 98-2112-M-007-028-MY3, 98-2119-M-002-007-MY3) and the Low Carbon Energy Research Center, National Tsing Hua University, Taiwan.

Received: February 3, 2012
Revised: February 27, 2012
Published online: April 2, 2012

[1] C. W. Tang, *Appl. Phys. Lett.* **1986**, *48*, 183.
[2] G. Yu, J. Gao, J. C. Hummelen, F. Wudl, A. J. Heeger, *Science* **1995**, *270*, 1789.
[3] G. Li, V. Shrotriya, J. S. Huang, Y. Yao, T. Moriarty, K. Emery, Y. Yang, *Nat. Mater.* **2005**, *4*, 864.
[4] Y. Kim, S. Cook, S. M. Tuladhar, S. A. Choulis, J. Nelson, J. R. Durrant, D. D. C. Bradley, M. Giles, I. Mcculloch, C. S. Ha, M. Ree, *Nat. Mater.* **2006**, *5*, 197.
[5] H. W. Lin, L. Y. Lin, Y. H. Chen, C. W. Chen, Y. T. Lin, S. W. Chiu, K. T. Wong, *Chem. Commun.* **2011**, *47*, 7872.
[6] L. Y. Lin, C. W. Lu, W. C. Huang, Y. H. Chen, H. W. Lin, K. T. Wong, *Org. Lett.* **2011**, *13*, 4962.
[7] G. Wei, X. Xiao, S. Wang, J. D. Zimmerman, K. Sun, V. V. Diev, M. E. Thompson, S. R. Forrest, *Nano Lett.* **2011**, *11*, 4261.
[8] R. Fitzner, E. Reinold, A. Mishra, E. Mena-Osteritz, H. Ziehlke, C. Körner, K. Leo, M. Riede, M. Weil, O. Tsaryova, A. Weiß, C. Uhrich, M. Pfeiffer, P. Bäuerle, *Adv. Funct. Mater.* **2011**, *21*, 897.
[9] V. Steinmann, N. M. Kronenberg, M. R. Lenze, S. M. Graf, D. Hertel, K. Meerholz, H. Bürckstümmer, E. V. Tulyakova, F. Würthner, *Adv. Energy Mater.* **2011**, *1*, 888.
[10] J. Xue, B. P. Rand, S. Uchida, S. R. Forrest, *Adv. Mater.* **2005**, *17*, 66.
[11] Y. Matsuo, Y. Sato, T. Niinomi, I. Soga, H. Tanaka, E. Nakamura, *J. Am. Chem. Soc.* **2009**, *131*, 16048.
[12] D. Wynands, M. Levichkova, K. Leo, C. Uhrich, G. Schwartz, D. Hildebrandt, M. Pfeiffer, M. Riede, *Appl. Phys. Lett.* **2010**, *97*, 073503.
[13] L. Y. Lin, Y. H. Chen, Z. Y. Huang, H. W. Lin, S. H. Chou, F. Lin, C. W. Chen, Y. H. Liu, K. T. Wong, *J. Am. Chem. Soc.* **2011**, *133*, 15822.
[14] S. W. Chiu, L. Y. Lin, H. W. Lin, Y. H. Chen, Z. Y. Huang, Y. T. Lin, F. Lin, Y. H. Liu, K. T. Wong, *Chem. Commun.* **2012**, *48*, 1857.
[15] Z. Chen, B. Cotterell, W. Wang, E. Guenther, S. J. Chua, *Thin Solid Films* **2001**, *394*, 202.
[16] J. M. Camacho, A. I. Oliva, *Thin Solid Films* **2006**, *515*, 1881.
[17] J. Y. Lee, S. T. Connor, Y. Cui, P. Peumans, *Nano Lett.* **2008**, *8*, 689.
[18] B. O'Connor, C. Haughn, K.-H. An, K. P. Pipe, M. Shtein, *Appl. Phys. Lett.* **2008**, *93*, 223304.
[19] S. R. Forrest, *Nature* **2004**, *428*, 911.
[20] T. Oyamada, Y. Sugawara, Y. Terao, H. Sasabe, C. Adachi, *Jpn. J. Appl. Phys.* **2007**, *46*, 1734.
[21] J. Meiss, M. K. Riede, K. Leo, *J. Appl. Phys.* **2009**, *105*, 063108.
[22] Z. C. Wu, Z. H. Chen, X. Du, J. M. Logan, J. Sippel, M. Nikolou, K. Kamaras, J. R. Reynolds, D. B. Tanner, A. F. Hebard, A. G. Rinzler, *Science* **2004**, *305*, 1273.
[23] M. W. Rowell, M. A. Topinka, M. D. McGehee, H. J. Prall, G. Dennler, N. S. Sariciftci, L. B. Hu, G. Gruner, *Appl. Phys. Lett.* **2006**, *88*, 233506.
[24] J. van de Lagemaat, T. M. Barnes, G. Rumbles, S. E. Shaheen, T. J. Coutts, C. Weeks, I. Levitsky, J. Peltola, P. Glatkowski, *Appl. Phys. Lett.* **2006**, *88*, 233503.
[25] J. B. Wu, H. A. Becerril, Z. N. Bao, Z. F. Liu, Y. S. Chen, P. Peumans, *Appl. Phys. Lett.* **2008**, *92*.
[26] J. Meiss, N. Allinger, M. K. Riede, K. Leo, *Appl. Phys. Lett.* **2008**, *93*, 103311.
[27] J. Meiss, M. K. Riede, K. Leo, *Appl. Phys. Lett.* **2009**, *94*, 013303.
[28] C.-F. Lin, S.-W. Liu, W.-F. Hsu, M. Zhang, T.-L. Chiu, Y. Wu, J.-H. Lee, *J. Phys. D: Appl. Phys.* **2010**, *43*, 395101.
[29] J. Meiss, M. Furno, S. Pfuetzner, K. Leo, M. Riede, *J. Appl. Phys.* **2010**, *107*, 053117.
[30] G. H. Jung, K. Hong, W. J. Dong, S. Kim, J.-L. Lee, *Adv. Energy Mater.* **2011**, *1*, 1023.
[31] J. Lee, S.-Y. Kim, C. Kim, J.-J. Kim, *Appl. Phys. Lett.* **2010**, *97*, 083306.
[32] B. O'Connor, K. H. An, K. P. Pipe, Y. Zhao, M. Shtein, *Appl. Phys. Lett.* **2006**, *89*, 233502.
[33] J. Meiss, K. Leo, M. K. Riede, C. Uhrich, W.-M. Gnehr, S. Sonntag, M. Pfeiffer, *Appl. Phys. Lett.* **2009**, *95*, 213306.
[34] Y.-C. Tseng, A. U. Mane, J. W. Elam, S. B. Darling, *Sol. Energy Mater. Sol. Cells* **2012**, *99*, 235.
[35] F. Liu, S. Shao, X. Guo, Y. Zhao, Z. Xie, *Sol. Energy Mater. Sol. Cells* **2010**, *94*, 842.
[36] L. A. A. Pettersson, L. S. Roman, O. Inganas, *J. Appl. Phys.* **1999**, *86*, 487.
[37] Z. Tang, L. M. Andersson, Z. George, K. Vandewal, K. Tvingstedt, P. Heriksson, R. Kroon, M. R. Andersson, O. Inganäs, *Adv. Mater.* **2012**, *24*, 554.